KJO
pISSN: 1011-8942 eISSN: 2092-9382

Korean J Ophthalmol 2022;36(5):379-389
https://doi.org/10.3341/kjo.2022.0050

Original Article

# The Correlation of Peripapillary and Juxtapapillary Choroidal Thickness in Healthy Subjects

Dong Hwan Son[1], Jinho Lee[2,3], Jeong-Ah Kim[3,4]

[1]*Department of Ophthalmology, Hallym University Chuncheon Sacred Heart Hospital, Hallym University College of Medicine, Chuncheon, Korea*
[2]*Hana Seoul Eye Center, Bucheon, Korea*
[3]*Department of Ophthalmology, Seoul National University College of Medicine, Seoul, Korea*
[4]*Department of Ophthalmology, Kangwon National University School of Medicine, Chuncheon, Korea*

**Purpose:** To evaluate the correlation between the two methods of measuring the choroidal thickness around the optic nerve head (ONH).

**Methods:** We conducted a cross-sectional study. Sixty-two eyes of 62 healthy subjects were included. Using spectral domain optical coherence tomography, a peripapillary circle scan (diameter of 3.5 mm) and 24 radial B-scan images centered on the Bruch's membrane opening (BMO) were obtained. Peripapillary choroidal thickness (PPCT) and juxtapapillary choroidal thickness (JPCT) were measured using circle and radial B-scan images, respectively. Correlation and agreements between values measured by two methods were analyzed. Factors associated with PPCT and JPCT, and the difference between the values measured by the two methods were evaluated.

**Results:** A total of 62 eyes of 62 healthy subjects were enrolled. Average PPCT and JPCT were 165.2 ± 50.1 and 139.7 ± 39.2 μm, respectively. The linear regression analysis showed a strong correlation between both measurements (PPCT vs. JPCT, $r^2$ = 0.900, $p$ < 0.001). PPCT and JPCT measurements showed good agreement in global and all six sectors (intraclass correlation coefficients >0.900). Bland-Altman plot showed good agreement between the two methods with a systematic deviation of 17.9 μm and a 95% limits of agreement (±1.96 standard deviation) of -9.6 to 60.5. In multivariate regression analysis, BMO area (β = -11.87, $p$ = 0.002) was the only factor significantly correlated with the difference between PPCT and JPCT, which showed a negative correlation. The difference between PPCT and JPCT measurements (PPCT - JPCT) showed a divergent tendency with decreasing BMO area size.

**Conclusions:** The two measures of choroidal thickness around the ONH were well correlated. However, the peripapillary choroid was generally thicker than the juxtapapillary choroid, especially in eyes with small BMO area.

**Key Words:** Choroid, Choroidal thickness, Juxtapapillary choroidal thickness, Peripapillary choroidal thickness

*Received:* April 28, 2022 *Final revision:* July 1, 2022
*Accepted:* July 22, 2022

Corresponding Author: Jeong-Ah Kim, MD. Department of Ophthalmology, Kangwon National University School of Medicine, 1 Gangwondaehak-gil, Chuncheon 24341, Korea. Tel: 82-33-240-5176, Fax: 82-33-255-6244, E-mail: dr.kimja@gmail.com

Vascular theory of glaucoma suggests that impaired perfusion of the optic nerve head (ONH) can directly expose the axons of retinal ganglion cells to ischemic damage or increase the susceptibility of glial and/or neural elements of the ONH to pressure-induced damage [1,2]. For this rea-

son, the choroidal vasculature within the parapapillary area has been of particular interest in understanding the pathogenesis of glaucoma in especially normal tension glaucoma (NTG) since it is downstream from the short posterior ciliary artery, which also perfuses the deep ONH structures [3-5]. Besides glaucoma, the pathognomic association between the choroid around ONH and nonarteritic anterior ischemic optic neuropathy (NAION) has been suggested, as this disease is most likely thought to be caused by transient hypoperfusion within the capillary bed of ONH, which is closely related to the choroidal vasculature [6-8]. Therefore, evaluation of the choroid around ONH would be critical in understanding the pathogenesis of not only glaucomatous optic neuropathy (GON) but also other non-GON.

However, study results of the correlation between the incidence and severity of GON and the peripapillary choroidal thickness seem to differ [6,8]. Even in studies of Korean NTG patients, the relationship between NTG and peripapillary choroidal thickness are not consistent [9,10]. This may be due to the differences in the patient group included in the study, but it may also be because measuring methods of choroidal thickness between studies are different. For this reason, it is essential to find out if there are agreements between the measurement methods or if there are factors that cause the difference. But to our knowledge, no studies have been conducted on the correlation between the measurements.

Among the methods evaluating choroid around ONH, measurement of peripapillary choroidal thickness (PPCT) and juxtapapillary choroidal thickness (JPCT) has been widely used [9-11]. Therefore, we evaluated correlations of the PPCT and JPCT, which are measured with the same center (Bruch's membrane opening, BMO), and analyzed the factors associated with the difference between the two measures.

## Materials and Methods

### Ethics statement

This study was approved by the Institutional Review Board of Kangwon National University Hospital (No. 2021-11-022). The study adhered to the tenets of the Declaration of Helsinki. Written consent was waived due to the retrospective study design.

### Subject selection

This study retrospectively analyzed the medical records of healthy subjects between 20 and 80 years of age at Kangwon National University Hospital (Chuncheon, Korea) between September 2021 and March 2022. Healthy control subjects were enrolled from patients who visited the clinic due to nonglaucomatous problem (e.g., incipient cataract, dry eye).

In the current study, subjects underwent ophthalmic examination, which included measurements of best-corrected visual acuity, refraction tests, slit-lamp biomicroscopy, intraocular pressure (IOP) measured by Goldmann applanation tonometry or Icare ic200 (Icare Finland Oy, Helsinki, Finland), gonioscopy, dilated stereoscopic examination of the optic disc, central corneal thickness (Noncon Robo Pachy SP-9000; Konan Medical, Kobe, Japan), axial length (IOL Master 500; Carl Zeiss, Jena, Germany), and spectral domain optical coherence tomography (SD-OCT; Spectralis OCT, Heidelberg Engineering, Heidelberg, Germany).

Systolic blood pressure (SBP) and diastolic blood pressure (DBP) were measured in the sitting position on the right upper arm with an automated oscillometric device at the time of SD-OCT exam. Ocular systolic perfusion pressure was defined as SBP - IOP at the time of SD-OCT exam and ocular diastolic perfusion pressure was defined as DBP - IOP. Mean arterial pressure was calculated as DBP + 1 / 3(SBP - DBP).

Healthy eyes were defined as those with no history of ocular symptoms, disease, or intraocular surgery except for uncomplicated cataract extraction: an IOP ≤21 mmHg, open angle on gonioscopic examination, an absence of glaucomatous optic disc appearance and retinal nerve fiber layer (RNFL) defects, and normal RNFL thickness profile on the OCT circumpapillary RNFL thickness measurement. Absence of a glaucomatous disc appearance was defined as an intact neuroretinal rim without peripapillary hemorrhages, notches, or localized pallor.

Exclusion criteria were (1) OCT images of insufficient quality (i.e., truncated B-scans and image quality <20) due to media opacity or lack of patient cooperation, (2) concomitant ocular disease (e.g., diabetic retinopathy, retinal vein occlusion, or optic neuropathies) or neurologic disease (e.g., pituitary tumor), (3) refractive error exceeding ±6.00

diopters (D) sphere or ±3.00 D astigmatism, and (4) OCT images which did not allow clear delineation of anterior and posterior border of the choroid. When both eyes of a subject were eligible, one eye was randomly selected.

## SD-OCT imaging around the peripapillary area

Two OCT scan patterns centered on BMO and aligned to the fovea were obtained by SD-OCT using Glaucoma Module Premium Edition ver. 1.0.16.0 (Heidelberg Engineering) which provides three circle B-scans (diameters of 3.5, 4.1, and 4.7 mm) for RNFL thickness along with 24 radial B-scans for BMO-minimum rim width (BMO-MRW). The corneal curvature of each eye was entered into the OCT system before performing SD-OCT scanning to compensate for potential magnification error. A light source of 870 nm was used according to standard imaging procedures. The scanning pattern was centered on the BMO with radial equidistance (24-high resolution 15° radial scans, each averaged from 27 B-scans). In this mode, the OCT device (Heidelberg Engineering) automatically detects BMO in 24-high resolution 15° radial scans of the ONH, each averaged from 20 to 30 individual B-scans, with 1,536 A-scans per B-scan acquired with scanning speed of 40,000 A-scans/sec [12,13]. Then, three circular scans along peripapillary circles (RNFL-BMO scanning) with diameters of 3.5, 4.1, and 4.7 mm (inner, middle, and outer, respectively) measure three sets of circumpapillary RNFL thicknesses (RNFLT) centered on BMO. Each scan circle produces a global average, and the mean thickness for each of the six sectors relative to the foveal-BMO axis, is as follows: superonasal (SN; 85°–125°), nasal (N; 125°–235°), inferonasal (IN; 235°–275°), inferotemporal (IT; 275°– 315°), temporal (T; 315°–45°), and superotemporal (ST; 45°–85°) [14].

The foveal-BMO axis was obtained automatically at the time of RNFL-BMO scanning. The foveal-BMO axis was defined as the angle between the fovea and BMO center relative to the horizontal axis of the image-acquisition frame. The device software automatically performs image segmentation, measurements, and classifications. The automatic segmentations were checked and corrected manually when necessary. The parameters exported for analysis were BMO area (BMOA), global averages of MRW and RNFLT, and the normative classification of global MRW and RNFLT. Well-centered scans with cor-

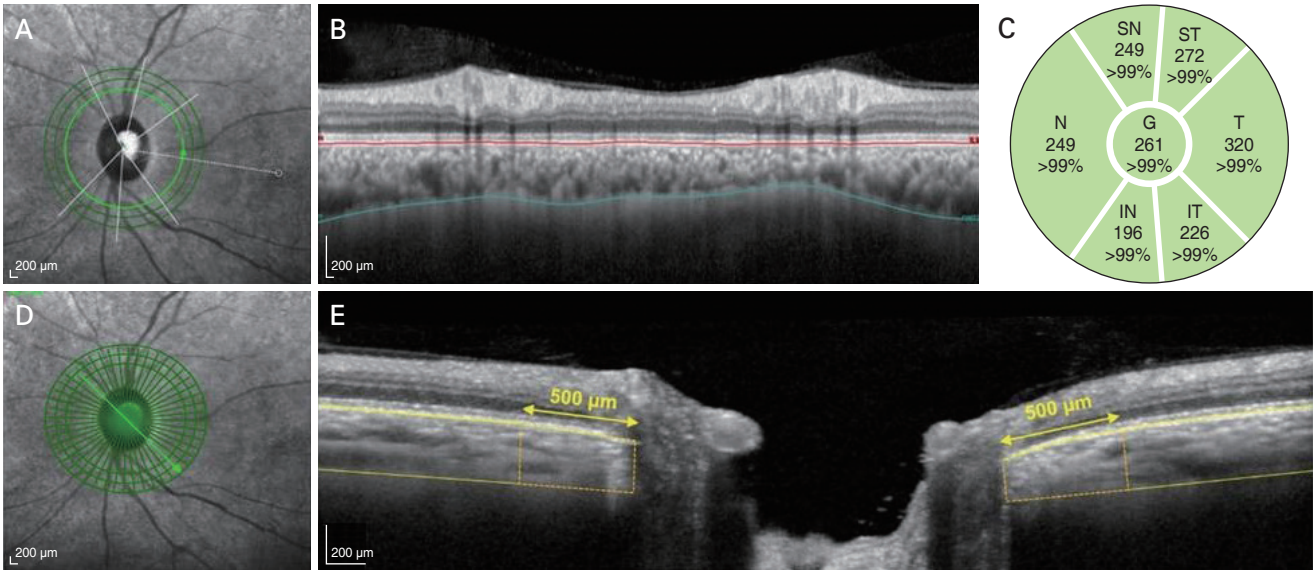


**Fig. 1.** Measurement of (A-C) peripapillary choroidal thickness (PPCT) and (D-E) juxtapapillary choroidal thickness (JPCT) using spectral domain optical coherence tomography (OCT). (A) Peripapillary 3.5-mm circular scan is obtained. (B) After delineating the posterior edge of the retinal pigment epithelium (red line) and the sclerochoroidal interface (blue line), (C) PPCT of the global (G) and the six sectors (superonasal [SN], nasal [N], inferonasal [IN], inferotemporal [IT], temporal [T], and superotemporal [ST]) were calculated by using the built-in software in the OCT system. (D) JPCT was measured at 48 meridians using the 24 radial scans centered on basement membrane opening. The area of the choroidal lumen within the 500 µm from the border tissue of Elschnig and the superior and inferior borders were defined manually by built-in caliper tool. (E) JPCT was calculated by dividing the measured choroidal area by 500 µm.

rect retinal segmentation and quality score of >20 were accepted. The BMOA was automatically calculated using the built-in software.

### Measurement of peripapillary choroidal thickness using SD-OCT

PPCT was measured using circular scans along peripapillary circles (RNFL-BMO scanning) with diameters of 3.5 mm with the manual segmentation function built-in the Heidelberg Eye Explorer ver. 1.0.16.0 (Heidelberg Engineering). Two experienced investigators (JAK and DHS), masked to the clinical information of participants, delineated the posterior edge of the retinal pigment epithelium and the sclerochoroidal interface, defined as the inner and outer boundaries of the choroid, respectively (Fig. 1A-1E). The average value measured by the two investigators was used for analysis. PPCT in corresponding sectors was determined automatically using the RNFL thickness algorithm function as follows: SN (85°–125°), N (125°–235°), IN (235°–275°), IT (275°– 315°), T (315°–45°), and ST (45°–85°) [14].

### Measurement of juxtapapillary choroidal thickness using 24 radial scans

JPCT was measured at 48 meridians using the 24 radial scans centered on BMO. In each meridian, the area of the choroidal lumen within the 500 μm from the border tissue of Elschnig was measured using built-in caliper tool. In eyes with oblique border tissue, the inner margin of the area of interest was determined at the innermost location at which the perpendicular distance between BMO and the choroidoscleral interface could be discerned. The superior and inferior borders were also defined manually by built-in caliper tool of the SD-OCT system (Fig. 1). Segmentation failures were corrected manually [15]. The JPCT was calculated by dividing the measured choroidal area by 500 μm. Measurements were performed by two investigators (JAK and DHS) masked to the participant's information and the study purpose, and the mean of the two measurements was considered for analysis. The mean JPCT was calculated using the mean of the 48 JPCT measurements. JPCT in corresponding sectors was determined by using the RNFL thickness algorithm function as follows: SN (85°–125°), N (125°–235°), IN (235°–275°), IT (275°– 315°), T (315°–45°), and ST (45°–85°) [14].

### Statistical analysis

The interobserver reproducibility in the measurement of the PPCT and JPCT was assessed by calculating intraclass correlation coefficients (ICCs). PPCT and JPCT were compared by linear regression models in global and six sectors. Intraeye comparisons of choroidal thickness were analyzed using paired *t*-tests, and a Bland-Altman plot was used to demonstrate the agreement. The raw data for *t*-tests were subjected to Bonferroni's correction based on the number of comparisons within each analysis. The correlation between the two measurements was assessed by the ICC. Factors associated with PPCT and JPCT were evaluated by univariate and multivariate analysis. Only variables with $p < 0.10$ on univariate analysis were included in the multivariate model. Factors associated with the difference between PPCT and JPCT were also evaluated in the same manner. Statistical significance was defined by a *p*-value of <0.05. Data were analyzed using IBM SPSS ver. 26.0 (IBM Corp., Armonk, NY, USA).

**Table 1.** Demographic characteristics of the study subjects (n = 62)

| Characteristic | Value |
|---|---|
| Age (yr) | 48.80 ± 17.60 |
| Female sex | 35 (56.5) |
| Diabetes mellitus | 9 (14.5) |
| Hypertension | 12 (19.4) |
| Baseline intraocular pressure (mmHg) | 13.00 ± 3.40 |
| Refractive error (D) | -1.08 ± 1.93 |
| Systolic blood pressure (mmHg) | 127.30 ± 15.50 |
| Diastolic blood pressure (mmHg) | 74.20 ± 8.90 |
| Mean arterial pressure (mmHg) | 91.90 ± 10.40 |
| Central corneal thickness (μm) | 547.70 ± 30.70 |
| Axial length (mm) | 24.68 ± 1.48 |
| Global RNFL thickness (μm) | 94.30 ± 9.40 |
| Visual field (dB) | |
| Mean deviation | -0.09 ± 1.55 |
| Pattern standard deviation | 1.37 ± 0.45 |
| Bruch's membrane opening area ($mm^2$) | 2.40 ± 0.50 |

Values are presented as mean ± standard deviation or number (%).
D = diopters; RNFL = retinal nerve fiber layer.

## Results

This study initially enrolled 71 healthy subjects. Nine of these subjects were excluded: five because the image quality of the OCT disc scans was too poor, which did not allow clear delineation of anterior and posterior border of the choroid; and four because of the refractive error exceeding -6.00 D sphere. Thus, a total of 62 eyes of 62 healthy subjects were enrolled. The clinical characteristics of participants are shown in Table 1. The mean age of participants was 48.8 ± 17.6 years, and 35 (56.5%) were female. The mean baseline IOP was 13.0 ± 3.4 mmHg. The refractive error showed a mean spherical equivalent of -1.08 ± 1.93 D. Mean axial length and global RNFLT (the inner circle) were 24.68 ± 1.48 mm and 94.3 ± 9.4μm, respectively. The mean value of BMOA was 2.4 ± 0.5 $mm^2$.

### Comparison of the PPCT and JPCT

Interobserver reproducibility was excellent in measuring PPCT (ICC, 0.998) and JPCT (ICC, 0.994). Table 2 and Fig. 2 show the measured PPCT and JPCT globally and in all six sectors. Global PPCT and JPCT were 165.2 ± 50.1 and 139.7 ± 39.2 μm, respectively. PPCT was generally thicker than JPCT in global and all sectors ($p < 0.001$ each).

**Table 2.** Comparison between PPCT and JPCT (n = 62)

| Variable | PPCT (μm) | JPCT (μm) | *p*-value* |
|---|---|---|---|
| Average | 165.2 ± 50.1 | 139.7 ± 39.2 | <0.001 |
| Superotemporal sector | 181.7 ± 58.5 | 150.4 ± 41.7 | <0.001 |
| Temporal sector | 162.7 ± 58.9 | 140.3 ± 44.3 | <0.001 |
| Inferotemporal sector | 139.2 ± 47.7 | 124.0 ± 39.5 | <0.001 |
| Inferonasal sector | 142.0 ± 48.2 | 128.1 ± 42.0 | <0.001 |
| Nasal sector | 172.3 ± 48.5 | 145.5 ± 39.4 | <0.001 |
| Superonasal sector | 181.7 ± 57.4 | 142.1 ± 41.3 | <0.001 |

Values are presented as mean ± standard deviation.
PPCT = peripapillary chorodial thickness; JPCT = juxtapapillary chorodial thickness.
*Calculated by paired *t*-test. The raw data for *t*-tests were subjected to Bonferroni correction based on the number of comparisons within each analysis. Values significant after Bonferroni correction ($p < 0.008$ [0.05/6]).

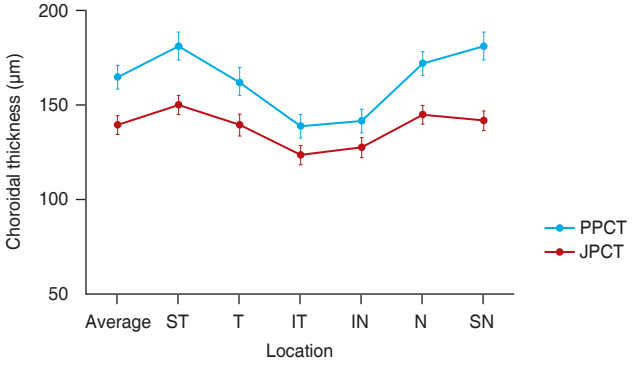


**Fig. 2.** Graph showing comparison of the global and sectoral peripapillary choroidal thickness (PPCT) and juxtapapillary choroidal thickness (JPCT) in healthy subjects. Note that PPCT is thicker than JPCT in global and all six sectors ($p < 0.001$ each). Dot and scale bar indicate the mean of the value and the standard error of mean, respectively. ST = superotemporal; T = temporal; IT = inferotemporal; IN = inferonasal; N = nasal; SN = superonasal.

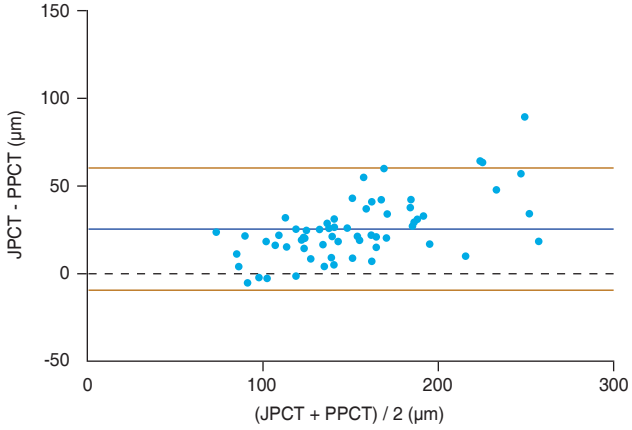


**Fig. 3.** Bland-Altman plot representing the difference between both measurement methods for global peripapillary choroidal thickness (PPCT) in healthy subjects: PPCT versus juxtapapillary choroidal thickness (JPCT). The red lines represent 95% limits of agreement. The mean difference between both groups was 25.4 with a standard deviation of 17.9.

**Table 3.** Intraclass correlation coefficient of peripapillary and juxtapapillary chorodial thickness (n = 62)

| Variable | Intraclass correlation coefficient | *p*-value* |
|---|---|---|
| Average | 0.959 | <0.001 |
| Superotemporal sector | 0.917 | <0.001 |
| Temporal sector | 0.953 | <0.001 |
| Inferotemporal sector | 0.931 | <0.001 |
| Inferonasal sector | 0.950 | <0.001 |
| Nasal sector | 0.942 | <0.001 |
| Superonasal sector | 0.908 | <0.001 |

*Statistically significant after correction of multiple comparisons using false discovery.

## Correlation between the PPCT and JPCT

Fig. 3 shows the Bland-Altman plot demonstrating the agreement between the global PPCT and JPCT. The agreement between the two methods was good with a systematic deviation of 17.9 μm and a 95% limits of agreement (±1.96 standard deviation) of -9.6 to 60.5. Also, the two methods showed good correlation in all divided sectors (global: ICC = 0.959, $p < 0.001$; ST: ICC = 0.917, $p < 0.001$; T: ICC = 0.953, $p < 0.001$; IT: ICC = 0.931, $p < 0.001$; IN: ICC = 0.950, $p < 0.001$; N: ICC = 0.942, $p < 0.001$; SN: ICC = 0.908, $p < 0.001$) (Table 3). The linear regression analysis between the two measurements is shown in Fig. 4A-4G. It shows a generally good correlation between both measurements (PPCT vs. JPCT) in global, and all six sectors (global:

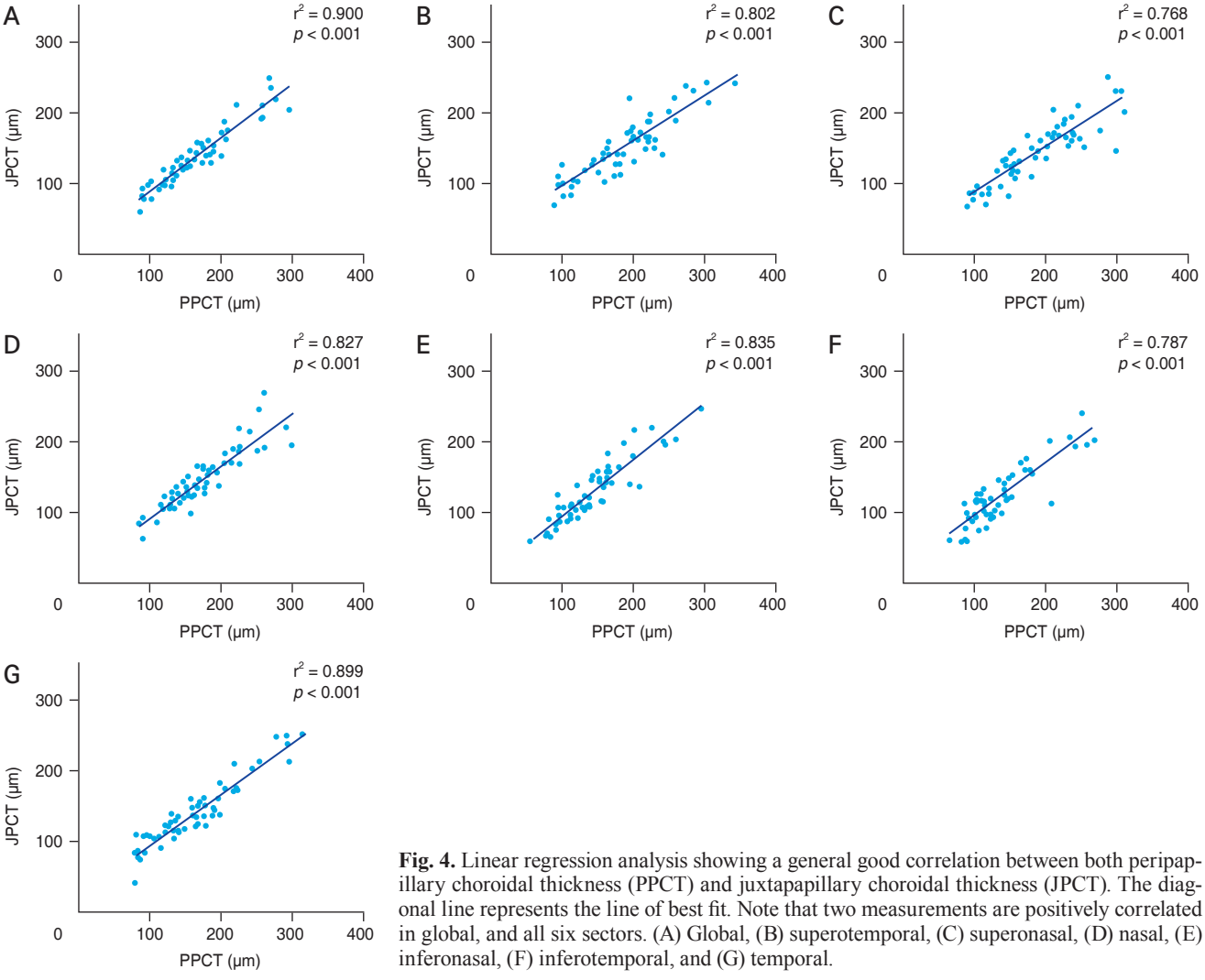


**Fig. 4.** Linear regression analysis showing a general good correlation between both peripapillary choroidal thickness (PPCT) and juxtapapillary choroidal thickness (JPCT). The diagonal line represents the line of best fit. Note that two measurements are positively correlated in global, and all six sectors. (A) Global, (B) superotemporal, (C) superonasal, (D) nasal, (E) inferonasal, (F) inferotemporal, and (G) temporal.

β = 0.74, $p < 0.001$; ST: β = 0.64, $p < 0.001$; T: β = 0.71, $p < 0.001$; IT: β = 0.73, $p < 0.001$; IN: β = 0.80, $p < 0.001$; N: β = 0.74, $p < 0.001$; SN: β = 0.63, $p < 0.001$).

## Factors associated with PPCT and JPCT

Linear regression analysis was performed to investigate factors associated with PPCT and JPCT (Table 4). In the univariate analysis, age showed a negative correlation with both PPCT (β = -0.97, $p = 0.006$) and JPCT (β = -0.82, $p = 0.005$), respectively. Also, BMOA showed a significant negative correlation with PPCT (β = -21.65, $p = 0.035$), whereas it did not show a statistically significant correlation with JPCT (β = -8.82, $p = 0.296$). In the multivariate analysis, PPCT was negatively correlated with age (β = -1.37, $p < 0.001$) and BMOA (β = -34.14, $p = 0.004$), but in case with JPCT, age was the only factor of significant correlation (β = -0.73, $p = 0.012$).

## Factors associated with the differences between the PPCT and JPCT

The linear regression analysis for the factors associated with the difference between the JPCT and PPCT (JPCT -

**Table 4.** Factors associated with PPCT and JPCT in healthy subjects (n = 62)

| Variable | PPCT | | | | JPCT | | | |
|---|---|---|---|---|---|---|---|---|
| | Univariate | | Multivariate | | Univariate | | Multivariate | |
| | β | *p*-value | β | *p*-value | β | *p*-value | β | *p*-value |
| Age (yr) | -0.97 | 0.006 | -1.37 | <0.001 | -0.82 | 0.005 | -0.73 | 0.012 |
| Female sex | 14.84 | 0.241 | - | - | 5.72 | 0.586 | - | - |
| Systolic blood pressure (mmHg) | -0.22 | 0.592 | - | - | -0.09 | 0.794 | - | - |
| Diastolic blood pressure (mmHg) | 0.32 | 0.639 | - | - | 0.42 | 0.459 | - | - |
| Mean arterial pressure (mmHg) | 0.27 | 0.956 | - | - | 0.35 | 0.734 | - | - |
| Spherical equivalent (D) | -1.52 | 0.642 | - | - | -1.30 | 0.632 | - | - |
| Central corneal thickness (μm) | -0.12 | 0.161 | - | - | -0.39 | 0.037 | -0.30 | 0.089 |
| Axial length (mm) | 2.37 | 0.588 | - | - | 3.51 | 0.330 | - | - |
| Global RNFL thickness (μm) | 0.31 | 0.651 | - | - | 0.29 | 0.606 | - | - |
| BMOA ($mm^2$) | -21.65 | 0.035 | -34.14 | 0.004 | -8.82 | 0.296 | - | - |

Only variables with $p < 0.10$ on univariate analysis were included in the multivariate model.
PPCT = peripapillary choroidal thickness; JPCT = juxtapapillary choroidal thickness; D = diopters; RNFL = retinal nerve fiber layer; BMOA = Bruch's membrane opening area.

**Table 5.** Factors associated with the difference between peripapillary and juxtapapillary choroidal thickness (n = 62)

| Variable | Univariate analysis | | Multivariate analysis | |
|---|---|---|---|---|
| | β | *p*-value | β | *p*-value |
| Age (yr) | -0.15 | 0.268 | - | - |
| Female sex | 6.54 | 0.092 | 7.01 | 0.052 |
| Systolic blood pressure (mmHg) | -0.13 | 0.395 | - | - |
| Diastolic blood pressure (mmHg) | -0.10 | 0.707 | - | - |
| Mean arterial pressure (mmHg) | -0.12 | 0.549 | - | - |
| Spherical equivalent (D) | -0.23 | 0.855 | - | - |
| Central corneal thickness (μm) | -0.03 | 0.375 | - | - |
| Axial length (mm) | -1.14 | 0.490 | - | - |
| Global RNFL thickness (μm) | 0.02 | 0.943 | - | - |
| Bruch's membrane opening area ($mm^2$) | -11.47 | 0.003 | -11.87 | 0.002 |

Only variables with $p < 0.10$ on univariate analysis were included in the multivariate model.
D = diopters; RNFL = retinal nerve fiber layer.

PPCT) is shown in Table 5. Based on the results of the univariate analysis, female sex (β = 6.54, $p$ = 0.092) and BMOA (β = -12.13, $p$ = 0.006) were included in the multivariate model. In a multivariate analysis of these two factors, BMOA (β = -11.87, $p$ = 0.002) was the only factor significantly correlated. Fig. 5. shows the association between BMOA and the difference between PPCT and JPCT, which shows a generally negative correlation.

## Discussion

The findings of this study demonstrate that the PPCT and JPCT values measured have a good agreement in global and all divided sectors and are well correlated. To the best of our knowledge, this is the first study to compare the measurement methods of the choroidal thickness around ONH.

In the current study, as both average and sectoral PPCT and JPCT values measured have a good correlation even though different measuring methods are used for each study, the measurements are expected to be similar. The measured average PPCT and JPCT of healthy subjects were 165.2 ± 50.1 and 139.7 ± 39.2 μm, respectively. These measurements are in line with the healthy control groups of the previous studies: JPCT in the study by Lee et al. [9] (135.56 ± 42.66 μm) and Lee et al. [16] (132.5 ± 41.8 μm), and PPCT in the study by Suh et al. [10] (140.60 ± 49.04 μm) and Hirooka et al. [17] (148.8 ± 53.3 μm).

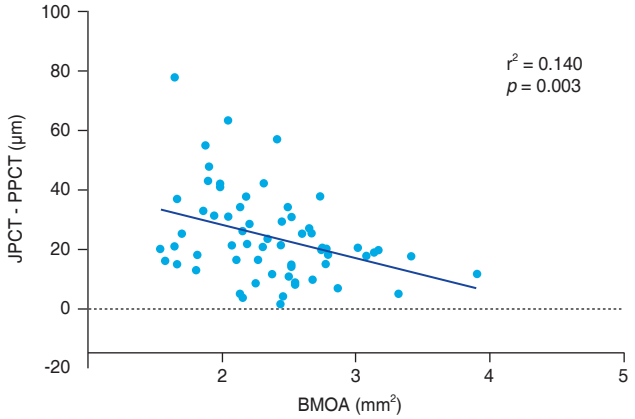


**Fig. 5.** Univariate linear regression showing a general good correlation between Bruch's membrane opening area (BMOA) and the difference between peripapillary chorodial thickness (PPCT) and juxtapapillary chorodial thickness (JPCT). The diagonal line represents the line of best fit. Note that BMOA and the difference between PPCT and JPCT is negatively correlated.

Many previous studies have reported that aging correlates with a thinner peripapillary choroid [9,18-22]. In the current study, both PPCT and JPCT showed a significant correlation with age. Age-related decline in PPCT and JPCT was -1.37 and -0.82 μm per year, respectively, similar to the rates reported in other studies [9,18-22].

In the present study, BMOA and PPCT showed a negative correlation (β = -21.65, $p$ = 0.035), whereas BMOA and JPCT did not show a statistically significant correlation (β = -8.82, $p$ = 0.296). Moreover, the difference between PPCT and JPCT measurements (PPCT - JPCT) showed a divergent tendency with decreasing BMOA size. The average BMOA of healthy subjects in our study were 2.4 ± 0.5 $mm^2$, which is comparable with Torres et al. [23] (1.8 ± 0.3 $mm^2$) and Amini et al. [24] (1.85 ± 0.45 $mm^2$). Because the peripapillary choroidal tissue shows a concentric pattern, increasing in thickness when increasing the distance from the optic nerve, the distance from the optic disc margin to the measurement site affects the measured choroidal thickness [25]. As PPCT is measured by peripapillary 3.5-mm circle scanning, the distance from optic disc margin to the measurement for the choroidal thickness would be affected by BMOA. In contrast, JPCT is measured based on the area of the choroid within the 500 μm from the border tissue of Elschnig, which is less affected by BMOA. Thus, the difference of the distance from the site of the choroidal thickness measurement to the optic disc margin caused by small BMOA should have caused the divergent tendency of the measurement differences of PPCT and JPCT. Although it is difficult to generalize this study because it was analyzed with a relatively small number of patients, JPCT seems to be a more suitable parameter to reduce the influence of the size of the optic disc in the study of choroid thickness analysis around the optic nerve. For PPCT, it would be better to match the optic disc size between groups. Further studies should consider this factor, in especially diseases with extremely smaller or larger optic disc size compared to normal healthy subjects, which can result in possible measurement bias.

Studies have been conducted on the association between the choroid around ONH and the pathogenesis of GON and non-GON, since peripapillary choroid shares circulation from the posterior ciliary arteries [26,27]. In NAION, which is characterized by small optic disc size, transient vascular insufficiency to the ONH has been known as im-

portant pathogenic event to this disease. Therefore, multiple studies have investigated the pathogenic association between the peripapillary choroid and NAION [6-8]. However, studies comparing choroidal thickness around ONH in eyes with NAION showed conflicting results. Nagia et al. [6] showed thicker PPCT in NAION and contralateral eyes compared with normal healthy eyes, suggesting that a thicker choroid could create a compartment syndrome within the ONH, in which the axons and their blood supply are strained with fluctuations in choroidal volume within the narrow central cup. However, Garcia-Basterra et al. [8] reported a significantly thinner PPCT in NAION and unaffected contralateral eyes, suggesting that a thin PPCT added to other predisposing factors for vascular insufficiency may reflect an optic nerve more vulnerable to choroidal circulation flow changes and more susceptible to transient hypoxia. These different results of choroidal thickness values may have been brought out because, as mentioned in our study, the difference between PPCT and JPCT is more significant in the eyes with smaller BMOA or ODA. Also, in the case of the study by Garcia-Basterra et al. [8], which has shown thinner PPCT in NAION compared with normal healthy eyes, NAION patients have a generally smaller optic disc size than normal control groups, but optic disc size comparison was not included in the study design. So, if normal subjects are set as the control group, the optic disc size of the disease group would be smaller than that of the control group. Consequently, peripapillary choroidal thickness values may have been affected and may have caused a bias in the measured choroidal thickness values. Thus, to investigate the relationship between NAION and choroidal thickness around ONH, further optic disc size or BMOA matched case-control studies with a large number of subjects will be needed.

Previous studies found an association between the longer axial length and the thinner peripapillary choroid in healthy eyes [17,19,28]. These findings suggest that the reduced choroidal circulation may lead to further degeneration of the choroid and retina in individuals with high myopia, which may cause the onset and progression of high myopia-related complications [29]. However, the current study did not show any significant correlation between the axial length and the choroidal thickness measured by two methods. Given our exclusion criteria for refractive error, we excluded highly myopic eyes. It seems that due to the narrow range of axial length, a significant correlation could not be confirmed. The relationship between PPCT, JPCT, and axial length might have been significant with the inclusion of highly myopic eyes.

Our study has several limitations. First, this study included a relatively small number of participants, all of which were Korean. Therefore, results may not be directly applicable to subjects of other ethnicities. Second, as our study is the first to compare measuring methods of choroidal thickness around ONH in only healthy subjects, further research is required in patients with GON or non-GON. Third, the current study evaluated association between BMOA and choroidal thickness around ONH and found no definite association between BMOA and JPCT. Because this study has a narrow BMOA range, we may not have been able to find the effect of BMOA on JPCT. Further studies with wide range of BMOA will be favorable. Fourth, the study by Lee et al. [16] have shown that parapapillary atrophy (PPA) with intact basement membrane is correlated with JPCT, and the influence of PPA could be associated with the thinning of the JPCT. Also, Sung et al. [30] showed a thinning tendency of the peripapillary choroid as the width of PPA became larger. β-PPA is presumed to be correlated with thinner peripapillary choroid. However, the primary goal of our study was to find out factors affecting the two measurement methods, so we did not take PPA into account.

In conclusion, the two choroidal thickness measures around the ONH in healthy subjects were well correlated. However, the peripapillary choroid was significantly thicker than the juxtapapillary choroid especially in eyes with small disc size (average BMOA). For this reason, researchers should consider that study results can vary due to different choroidal thickness measurements, especially in studies of diseases of small disc size.

**Conflicts of Interest:** None.
**Acknowledgements:** None.
**Funding:** This research was supported by a grant of Patient-Centered Clinical Research Coordinating Center funded by the Korean government (the Ministry of Health and Welfare) (No. HI19C0481 and HC19C0276).

## References

1. Nicolela MT, Ferrier SN, Morrison CA, et al. Effects of

cold-induced vasospasm in glaucoma: the role of endothelin-1. *Invest Ophthalmol Vis Sci* 2003;44:2565-72.
2. Mojon DS, Hess CW, Goldblum D, et al. High prevalence of glaucoma in patients with sleep apnea syndrome. *Ophthalmology* 1999;106:1009-12.
3. Lee EJ, Lee KM, Lee SH, Kim TW. OCT angiography of the peripapillary retina in primary open-angle glaucoma. *Invest Ophthalmol Vis Sci* 2016;57:6265-70.
4. Lee EJ, Lee KM, Lee SH, Kim TW. Parapapillary choroidal microvasculature dropout in glaucoma: a comparison between optical coherence tomography angiography and indocyanine green angiography. *Ophthalmology* 2017;124:1209-17.
5. Lee EJ, Lee SH, Kim JA, Kim TW. Parapapillary deep-layer microvasculature dropout in glaucoma: topographic association with glaucomatous damage. *Invest Ophthalmol Vis Sci* 2017;58:3004-10.
6. Nagia L, Huisingh C, Johnstone J, et al. Peripapillary pachychoroid in nonarteritic anterior ischemic optic neuropathy. *Invest Ophthalmol Vis Sci* 2016;57:4679-85.
7. Sharma S, Ang M, Najjar RP, et al. Optical coherence tomography angiography in acute non-arteritic anterior ischaemic optic neuropathy. *Br J Ophthalmol* 2017;101:1045-51.
8. Garcia-Basterra I, Lahrach I, Morillo Sanchez MJ, et al. Analysis of peripapillary choroidal thickness in non-arteritic anterior ischaemic optic neuropathy. *Br J Ophthalmol* 2016;100:891-6.
9. Lee KM, Lee EJ, Kim TW. Juxtapapillary choroid is thinner in normal-tension glaucoma than in healthy eyes. *Acta Ophthalmol* 2016;94:e697-708.
10. Suh W, Cho HK, Kee C. Evaluation of peripapillary choroidal thickness in unilateral normal-tension glaucoma. *Jpn J Ophthalmol* 2014;58:62-7.
11. Kim JA, Son DH, Lee EJ, et al. Intereye comparison of the characteristics of the peripapillary choroid in patients with unilateral normal-tension glaucoma. *Ophthalmol Glaucoma* 2021;4:512-21.
12. Chauhan BC, O'Leary N, AlMobarak FA, et al. Enhanced detection of open-angle glaucoma with an anatomically accurate optical coherence tomography-derived neuroretinal rim parameter. *Ophthalmology* 2013;120:535-43.
13. Danthurebandara VM, Sharpe GP, Hutchison DM, et al. Enhanced structure-function relationship in glaucoma with an anatomically and geometrically accurate neuroretinal rim measurement. *Invest Ophthalmol Vis Sci* 2014;56:98-105.
14. Lee EJ, Lee KM, Kim H, Kim TW. Glaucoma diagnostic ability of the new circumpapillary retinal nerve fiber layer thickness analysis based on Bruch's membrane opening. *Invest Ophthalmol Vis Sci* 2016;57:4194-204.
15. Mansouri K, Medeiros FA, Tatham AJ, et al. Evaluation of retinal and choroidal thickness by swept-source optical coherence tomography: repeatability and assessment of artifacts. *Am J Ophthalmol* 2014;157:1022-32.
16. Lee SH, Lee EJ, Kim TW. Topographic correlation between juxtapapillary choroidal thickness and microstructure of parapapillary atrophy. *Ophthalmology* 2016;123:1965-73.
17. Hirooka K, Tenkumo K, Fujiwara A, et al. Evaluation of peripapillary choroidal thickness in patients with normal-tension glaucoma. *BMC Ophthalmol* 2012;12:29.
18. Johnstone J, Fazio M, Rojananuangnit K, et al. Variation of the axial location of Bruch's membrane opening with age, choroidal thickness, and race. *Invest Ophthalmol Vis Sci* 2014;55:2004-9.
19. Rhodes LA, Huisingh C, Johnstone J, et al. Peripapillary choroidal thickness variation with age and race in normal eyes. *Invest Ophthalmol Vis Sci* 2015;56:1872-9.
20. Huang W, Wang W, Zhou M, et al. Peripapillary choroidal thickness in healthy Chinese subjects. *BMC Ophthalmol* 2013;13:23.
21. Roberts KF, Artes PH, O'Leary N, et al. Peripapillary choroidal thickness in healthy controls and patients with focal, diffuse, and sclerotic glaucomatous optic disc damage. *Arch Ophthalmol* 2012;130:980-6.
22. Yang H, Luo H, Gardiner SK, et al. Factors influencing optical coherence tomography peripapillary choroidal thickness: a multicenter study. *Invest Ophthalmol Vis Sci* 2019;60:795-806.
23. Torres LA, Sharpe GP, Hutchison DM, et al. Influence of Bruch's membrane opening area in diagnosing glaucoma with neuroretinal parameters from optical coherence tomography. *Am J Ophthalmol* 2019;208:94-102.
24. Amini N, Miraftabi A, Henry S, et al. The relationship of the clinical disc margin and Bruch's membrane opening in normal and glaucoma subjects. *Invest Ophthalmol Vis Sci* 2016;57:1468-75.
25. Kadziauskiene A, Kuoliene K, Asoklis R, et al. Changes in choroidal thickness after intraocular pressure reduction following trabeculectomy. *Acta Ophthalmol* 2016;94:586-91.
26. Suh MH, Zangwill LM, Manalastas PI, et al. Deep retinal layer microvasculature dropout detected by the optical coherence tomography angiography in glaucoma. *Ophthal-*

*mology* 2016;123:2509-18.

27. Spalton DJ. Microvasculature of the human optic nerve. *Am J Ophthalmol* 1996;121:452-3.
28. Jiang R, Wang YX, Wei WB, et al. Peripapillary choroidal thickness in adult Chinese: the Beijing eye study. *Invest Ophthalmol Vis Sci* 2015;56:4045-52.
29. Song A, Hou X, Zhuo J, Yu T. Peripapillary choroidal thickness in eyes with high myopia. *J Int Med Res* 2020;48: 300060520917273.
30. Sung MS, Heo H, Piao H, et al. Parapapillary atrophy and changes in the optic nerve head and posterior pole in high myopia. *Sci Rep* 2020;10:4607.